ACS APPLIED MATERIALS & INTERFACES

Research Article

www.acsami.org

Versatile Wedge-Based System for the Construction of Unidirectional Collagen Scaffolds by Directional Freezing: Practical and Theoretical Considerations

Michiel W. Pot,*[,†] Kaeuis A. Faraj,[†,§] Alaa Adawy,[‡,∥] Willem J. P. van Enckevort,[‡] Herman T. B. van Moerkerk,[†] Elias Vlieg,[‡] Willeke F. Daamen,[†] and Toin H. van Kuppevelt[†]

[†]Department of Biochemistry 280, Radboud Institute for Molecular Life Sciences, Radboud university medical center, P.O. Box 9101, 6500 HB Nijmegen, The Netherlands

[‡]Department of Solid State Chemistry, Institute for Molecules and Materials, Radboud University Nijmegen, 6525 AJ Nijmegen, The Netherlands

Supporting Information

ABSTRACT: Aligned unidirectional collagen scaffolds may aid regeneration of those tissues where alignment of cells and extracellular matrix is essential, as for instance in cartilage, nerve bundles, and skeletal muscle. Pores can be introduced by ice crystal formation followed by freeze-drying, the pore architecture reflecting the ice crystal morphology. In this study we developed a wedge-based system allowing the production of a wide range of collagen scaffolds with unidirectional pores by directional freezing. Insoluble type I collagen suspensions were frozen using a custom-made wedge system, facilitating the formation of a horizontal as well as a vertical temperature gradient and providing a controlled solidification area for ice dendrites. The system permitted the growth of aligned unidirectional ice crystals over a large distance (>2.5 cm), an insulator prolonging the freezing process and facilitating the construction of crack-free scaffolds. Unidirectional collagen scaffolds with tunable pore sizes and pore morphologies were constructed by varying freezing rates and suspension media. The versatility of the system was indicated by the construction of unidirectional scaffolds from albumin, poly(vinyl alcohol) (a synthetic polymer), and collagen-polymer blends producing hybrid scaffolds. Macroscopic observations, temperature measurements, and scanning electron microscopy indicated that directed horizontal ice dendrite formation, vertical ice crystal nucleation, and evolutionary selection were the basis of the aligned unidirectional ice crystal growth and, hence, the aligned unidirectional pore structure. In conclusion, a simple, highly adjustable freezing system has been developed allowing the construction of large (hybrid) bioscaffolds with tunable unidirectional pore architecture.

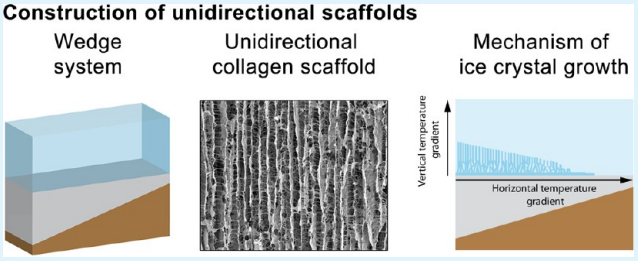

KEYWORDS: *regenerative medicine, biomaterials, lyophilization, anisotropy, collagen*

1. INTRODUCTION

Tissue engineering and regenerative medicine aim to restore the structure and function of damaged tissues and organs. A commonly used strategy is the incorporation of cells and effector molecules into supporting structures, also referred to as scaffolds, to induce tissue regeneration. An important parameter for the guidance of tissue formation is the pore architecture of scaffolds. Typical isotropic scaffolds show uniformity in all orientations, but isotropy may be undesirable in tissues displaying an anisotropic extracellular matrix (ECM). In this case, application of isotropic scaffolds may result in structural and mechanical discordance with the surrounding tissue, and the use of scaffolds with anisotropic architecture is therefore favored.[1]

Construction of unidirectional scaffolds has been widely investigated, since they provide cues to direct growth of tissues along the aligned structures.[2−4] Aligned growth is important during, e.g., the formation of nerve bundles, skeletal muscle fibers, and cartilaginous tissue. In addition, longitudinal microchannels have been reported to increase cellular influx.[5] Anisotropic pore organization in scaffolds has been applied for the regeneration of a number of tissues, such as intervertebral disc,[6] cartilage,[7] muscle,[8] tendon,[9] and nerves.[10] Besides the pore orientation, physical parameters as intrinsic surface topographies influence cellular behavior.[11]

ECM proteins are appropriate substrates for scaffolding material because of their biocompatibility, biodegradability, bioactive properties, and, in case of collagen, low antigenicity. Type I collagen is the most abundant scaffolding material in the body, and can be used to construct scaffolds of different architectures.[12] Several methods have been developed to produce anisotropic unidirectional porous collagen-based scaffolds,

Received: January 7, 2015
Accepted: March 30, 2015
Published: March 30, 2015

DOI: 10.1021/acsami.5b00169
ACS Appl. Mater. Interfaces 2015, 7, 8495−8505

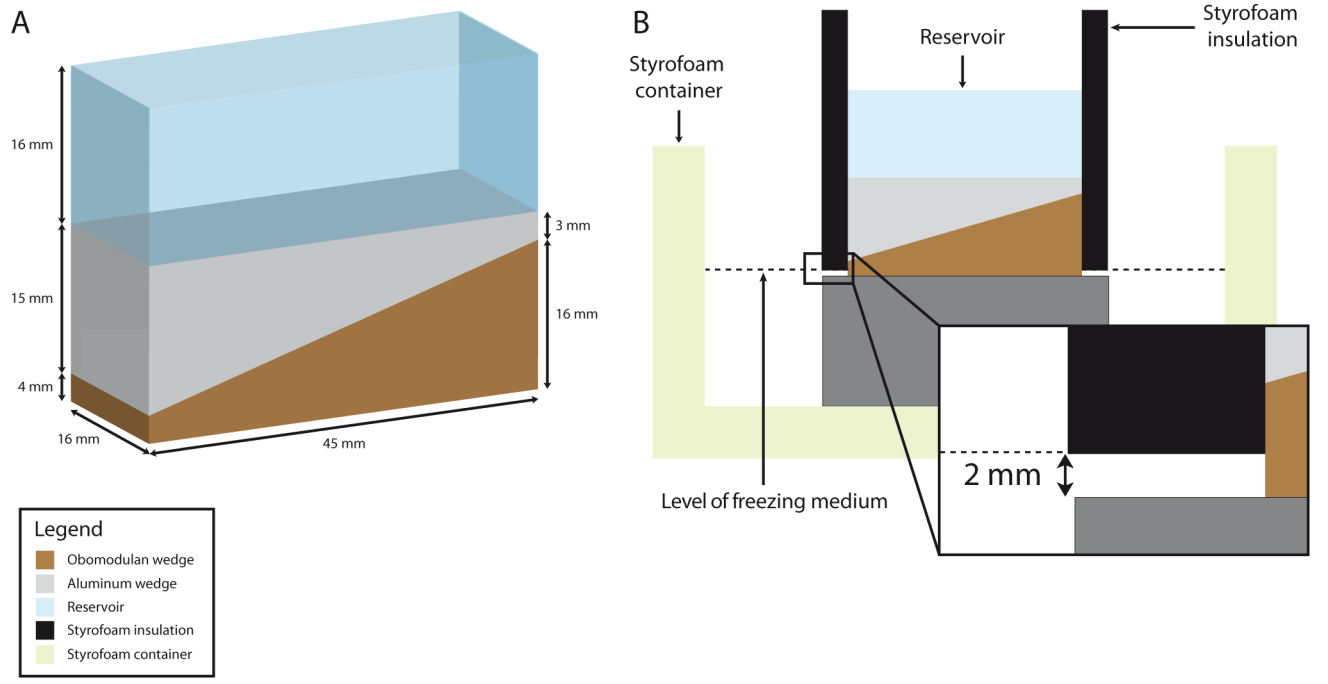

Figure 1. Experimental setup of the wedge system to construct unidirectional scaffolds. (A) Wedge system used for the preparation of lyophilized unidirectional scaffolds. The gray and brown wedges represent aluminum and Obomodulan, respectively. The suspension is present in the blue reservoir made from Scotch tape. (B) Front view of the wedge system in its experimental setup. The wedge system is placed on a plateau of aluminum in a styrofoam container. Styrofoam insulation surrounds the wedge system. The freezing medium is in direct contact with the wedge-shaped Obomodulan but not with the wedge-shaped aluminum.

such as lyophilization,[13] electrospinning,[14] and application of electrochemical gradients[15] and magnetic fields.[16] The requirement for complex equipment restricts wide applicability of most of these strategies. Moreover, many techniques require harsh operating conditions that can limit the use of biologicals, and the remaining organic solvents may cause in vivo toxicity.[17] From these techniques, lyophilization is a widely established method.[18] The pore architecture of scaffolds obtained by lyophilization reflects the ice crystal morphology obtained during freezing. Controlled growth of ice crystals forms the basis of the development of collagen scaffolds with a unidirectional structure and the final pore structure can be modified by adjusting the freezing regime.[12] Generally, comprehensive setups are employed to obtain unidirectional scaffolds by lyophilization.[19] For those studies reporting simple freezing strategies, one strategy is to dip collagen suspensions in freezing media,[20] which may limit control over the freezing process. Another simple approach is to fill a mold with collagen suspension and subsequently cool the mold with freezing media. Such simple molds typically consist of a metal surface and isolation, but generally result in limited homogeneity due to the lack of constant slow cooling.[21] To our knowledge the construction of collagen scaffolds with unidirectional pores over long distances (>2.5 cm) by controlled unidirectional freezing conditions have not been described before. The development of a simple adjustable system for the production of high quality tailor-made unidirectional collagen scaffolds may allow easy access to unidirectional scaffolds. Porous collagen scaffolds generally have rather weak mechanical strength. An improvement of (unidirectional) collagen scaffolds would be an increase in mechanical strength, such as tensile strength, fracture strength, and compressive strength. Reinforced hybrid scaffolds prepared from premixed collagen and water-soluble polymers such as poly(vinyl alcohol) may aid interesting characteristics for tissue engineering applications.[22] In this study, we describe an adjustable directional freezing method to develop porous collagen scaffolds with aligned unidirectional pores, taking into account the physics of ice crystal growth. A custom-made wedge system was developed to aid controlled solidification, especially in the initial phases of the freezing process. The influence of freezing temperature, solvents, collagen concentration, and use of synthetic polymers are described.

2. EXPERIMENTAL SECTION

2.1. Preparation of Scaffolds with Aligned Pores. Fibrillar insoluble type I collagen was isolated from bovine achilles tendon. The general procedure for scaffold construction comprised the preparation of a 0.7% (w/v) collagen suspension by incubating collagen fibrils overnight at 4 °C in 0.25 M acetic acid (pH 2.7, Scharlau, Spain). The collagen suspension was homogenized on ice using a Teflon glass Potter-Elvehjem device (Louwers Glass and Ceramic Technologies, Hapert, The Netherlands) with an intervening space of 0.35 mm (10 strokes). Air bubbles were removed by centrifugation at 117*g* for 30 min at 4 °C. Unidirectional porous collagen scaffolds were produced by directional freezing of the collagen suspension using a custom-made wedge system (for an overview of the system, including dimensions, see Figure 1).

The system consisted of two wedges of anodized aluminum and polyurethane (Obomodulan, type 652, Vink, Didam, The Netherlands) with thermal conductivities of 205 and 0.03 W/m·K, respectively. A 16 mm high reservoir of Scotch tape was attached to the aluminum wedge. Styrofoam insulation (outer dimensions: $W \times L \times H$ (mm): $45 \times 70 \times 40$; inner dimensions: $W \times L \times H$ (mm): $15 \times 45 \times 40$) was placed around the wedge system and reservoir to ensure a vertical temperature gradient without external disturbances. The wedge system was applied to induce a horizontal temperature gradient (see Figure 2B). The collagen suspension was pipetted into the reservoir. The wedge system was placed on a plateau of aluminum in a container, and the

DOI: 10.1021/acsami.5b00169
ACS Appl. Mater. Interfaces 2015, 7, 8495−8505

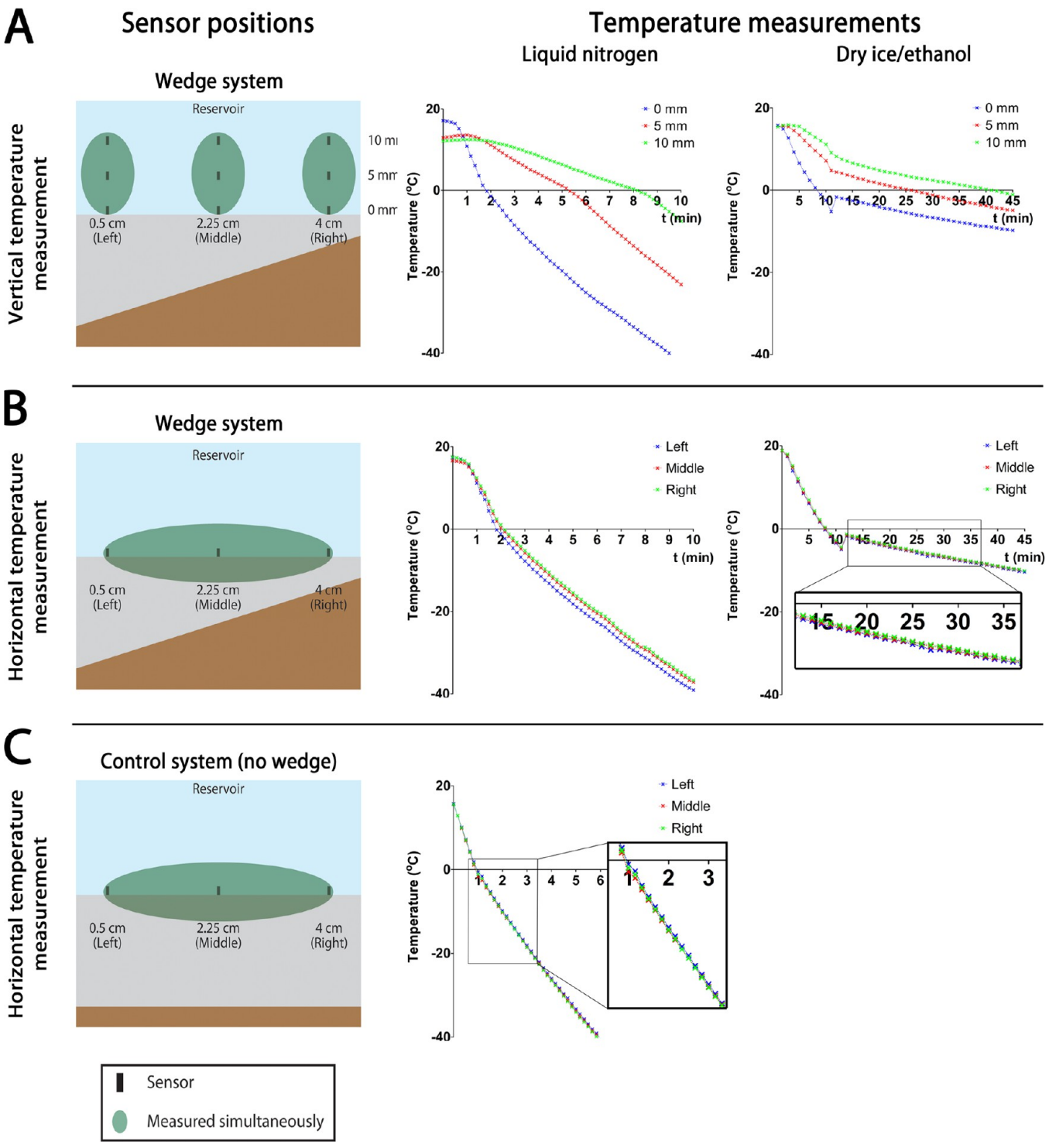

Figure 2. Experimental setup of the wedge system to construct unidirectional scaffolds. Temperature gradients observed during construction of unidirectional scaffolds using the wedge system. Liquid nitrogen or dry ice/ethanol were used as freezing medium. The position of the sensors is indicated. See Figure 1 for color coding of the wedge system. Data from representative measurements are shown. (A) Vertical temperature gradient with cooling rates of 6.4 ± 1.2 and 0.3 ± 0.1 °C/min for liquid nitrogen and dry ice/ethanol, respectively. (B) Horizontal temperature gradient measured during the entire freezing process. The temperature difference between the left and right sensor was 1.1 ± 0.9 °C ($p < 0.0001$) and 0.3 ± 0.1 °C ($p < 0.0001$) for −196 and −78 °C, respectively. (C) Horizontal temperature measurements performed using a nonwedge system indicated no obvious temperature differences between the left, middle, and right part of the wedge.

collagen suspension was subsequently frozen using liquid nitrogen (−196 °C). The freezing medium was only in contact with Obomodulan and not with the aluminum (Figure 1B). The system was left at ambient temperature during freezing. Scaffolds were prepared by freezing 10 mL of a collagen suspension followed by lyophilization for 2 days in a Zirbus freeze-dryer (Sublimator 500 II, Bad Grund, Germany). Next, scaffolds were stabilized using vapor fixation with 37% formaldehyde under vacuum for 30 min.[5]

The effect of different parameters on the pore structure was investigated, i.e., freezing temperature, collagen concentration, acetic

DOI: 10.1021/acsami.5b00169
ACS Appl. Mater. Interfaces 2015, 7, 8495−8505

acid concentration, addition of detergent, use of other components than collagen, and collagen/PVA blends (see Table 1).

Table 1. Overview of Parameters Examined and Results Obtained with Respect to Pore Size/Structure

parameters	results
freezing temperature: liquid nitrogen dry ice/ethanol	pore size smaller for lower freezing temperatures
collagen concentration: 0.4−2.0% (w/v)	pore size smaller for increased collagen concentration
detergent: no 15 mM octyl *p*-D-glycopyranoside	pore size smaller by incorporation of a detergent
acetic acid concentration: 0- 2 M	pore size larger and wall structure more closed for increased acetic acid concentration
(bio)molecule: bovine serum albumin polyvinyl alcohol collagen + polyvinyl alcohol	unidirectional scaffolds with morphology dependent on type and concentration of molecule

To investigate the effect of the freezing temperature and speed, the collagen suspension was also frozen using a mixture of dry ice and ethanol (−78 °C).

To study the effect of the volume of the applied collagen suspension, scaffolds were made using volumes up to 30 mL collagen suspension in 0.25 M acetic acid. Additional Scotch tape was attached to the wedge system for a 32 mm high reservoir.

To examine the effect of collagen concentration on pore structure, collagen suspensions of 0.4, 1.0, and 2.0% (w/v) were used. Collagen suspensions of 0.4% and 1% (w/v) were prepared similarly as 0.7% (w/v) while the 2.0% (w/v) collagen suspensions were homogenized by passing the suspension five times through a 50 mL syringe, followed by centrifugation at 2538*g* for 45 min to remove air bubbles.

To investigate the effect of a lowered surface free energy during ice crystal formation, a solution of 15 mM octyl β-D-glucopyranoside (Sigma-Aldrich), a nonionic detergent, in 0.25 M acetic acid was prepared, after which collagen fibrils were added.

The effect of the suspension medium was further studied by altering the concentration of the acetic acid used. Preparation of collagen in 0.025 M acetic acid (0.15 wt %, pH 3.5), 0.25 M acetic acid (1.5 wt %, pH 2.7), and 2 M acetic acid (12 wt %, pH 2.5) were studied. As a reference, collagen fibrils were suspended in Milli-Q water.

To investigate the versatility of the system for use of components other than collagen, scaffolds were prepared from 7% (w/v) bovine serum albumin (BSA, PAA Laboratories GmbH, Pasching, Austria) and 5, 10, 15, and 20% (w/v) poly(vinyl alcohol) (PVA, Sulkey of America, Kennesaw, GA, USA), all in 0.25 M acetic acid. Moreover, to investigate reinforcement of collagen scaffolds with synthetic polymers (hybrid scaffolds), mixtures of collagen and PVA (0.7% w/v collagen combined with 0.5, 1.0, 2.5, and 5.0% (w/v) PVA), in 0.25 M acetic acid, were prepared. All suspensions were homogenized using the Potter-Elvehjem device.

2.2. Process of Directional Solidification. The process of planar ice dendrite formation was visualized by video capture using a Sony Cybershot DSC-H10 camera. To visualize the process, 10 mL of a solution of 0.25 M acetic acid was frozen using liquid nitrogen. A solution without collagen was used to circumvent interference caused by the cloudy appearance of the collagen suspension.

Temperature measurements were performed to characterize the freezing process. The temperature differences in the collagen suspension during the freezing process with liquid nitrogen and a mixture of dry ice and ethanol were measured $n = 3$, in triplicate, at nine different locations (Figure 2B) using thermocouples (Testo 922 and 925, Testo AG, Lenzkirch, Germany). Sensors were placed at three locations on the aluminum surface, from the thick aluminum part to the thin aluminum part (left: 0.5 cm, middle: 2.25 cm, right: 4 cm). Sensors were also placed at three heights from the surface of the aluminum (bottom: 0 mm, middle: 5 mm, top: 10 mm) at three different locations (left: 0.5 cm, middle: 2.25 cm, right: 4 cm). As a control, sensors were placed on the aluminum surface (left: 0.5 cm, middle: 2.25 cm, right: 4 cm) of a nonwedge, flat system (aluminum: $W \times L \times H$ (mm): 15 × 45 × 15; Obomodulan: $W \times L \times H$ (mm): 15 × 45 × 3), and measurements were performed during freezing with liquid nitrogen. Temperature measurements were performed for 10 min with time intervals of 10 s for freezing at −196 °C and for 45 min with 1 min time intervals for freezing at −78 °C. The duration of the freezing process was measured from the start of the measurement until collagen suspensions were macroscopically frozen. Freezing times are represented as mean ± standard deviation (min). Cooling rates were calculated from 0 until −20 °C for temperature measurements at different heights. Cooling rates are represented as mean ± standard deviation (°C/min). Horizontal temperature differences between the left and the right sensor were calculated from 0 until −30 °C and are represented as mean ± standard deviation. The measured temperature difference between the left and the right sensor was divided by the distance between both sensors (3.5 cm) to calculate the temperature difference per cm (°C/cm).

2.3. Scaffold Morphology. The morphology of the scaffolds was evaluated using scanning electron microscopy (JEOL SEM6340F, Tokyo, Japan). Samples were mounted on stubs and sputtered with a thin layer of gold using a Polaron E5100 Coating System.[23] Images were recorded using an accelerating voltage of 10 kV. Scaffolds were cut longitudinally and perpendicularly. High magnification images were taken from the lower parts of scaffolds to assess the development of unidirectional pores. Pilot experiments showed homogeneity in pore size distribution throughout the scaffolds. In a pilot study three scaffolds were extensively analyzed with respect to pore size. The following data were obtained from nine samples per scaffold at three locations, left, middle, right (see Figure 2), and heights, 2, 6, and 10 mm. Pore sizes were 54 ± 9, 50 ± 9, and 55 ± 9 μm. On the basis of these data we used one longitudinal and cross-section per scaffold for further analysis. Four images were recorded from random locations per cross-section and the lengths of the shortest axis of 50 pores were measured using ImageJ. This experiment was performed $n = 3$ in triplicate.

2.4. Statistics. Statistical analyses were performed using GraphPad Prism (GraphPad Software, Inc., version 5, La Jolla, CA, U.S.A.). Horizontal temperature differences between the left and the right sensor were determined by paired *t* tests. The effect of the various experimental conditions was assessed by a repeated measures ANOVA with Tukey's posthoc test. Pore sizes are shown as mean ± standard deviation. P-values <0.05 were considered statistically significant.

3. RESULTS

3.1. Construction of Unidirectional Collagen Scaffolds. Collagen scaffolds with unidirectional pore architecture were constructed by directional freezing using the custom-made wedge system (Figure 1). The system consists of two opposite wedges of aluminum (upper layer) and Obomodulan (lower layer) that differ in thermal conductivity. The Obomodulan wedge is a poor thermal conductor, acting as a mediator between the freezing medium and the aluminum wedge, resulting in slower freezing compared to the situation when the aluminum layer would be in direct contact with liquid nitrogen. After completion of the freezing process, frozen suspensions could easily be removed from the Scotch tape reservoir. No cracks were observed before or after lyophilization.

Temperature measurements during the freezing process indicated a large vertical temperature gradient (Figure 2), resulting in freezing of the collagen suspension from the aluminum surface upward to where the collagen suspension was exposed to ambient temperature. Freezing at −196 and −78 °C resulted in cooling rates of 6.4 ± 1.2 and 0.3 ± 0.1 °C/min, respectively. Collagen suspensions were frozen after 11 ± 1 and 50 ± 5 min for freezing at −196 and −78 °C, respectively. Macroscopic observations showed that the wedge system induced horizontal dendrite formation by the growth of ice dendrites over the aluminum surface of the wedge (Supporting Information 1, video). To evaluate the presence of a horizontal

DOI: 10.1021/acsami.5b00169
ACS Appl. Mater. Interfaces 2015, 7, 8495−8505

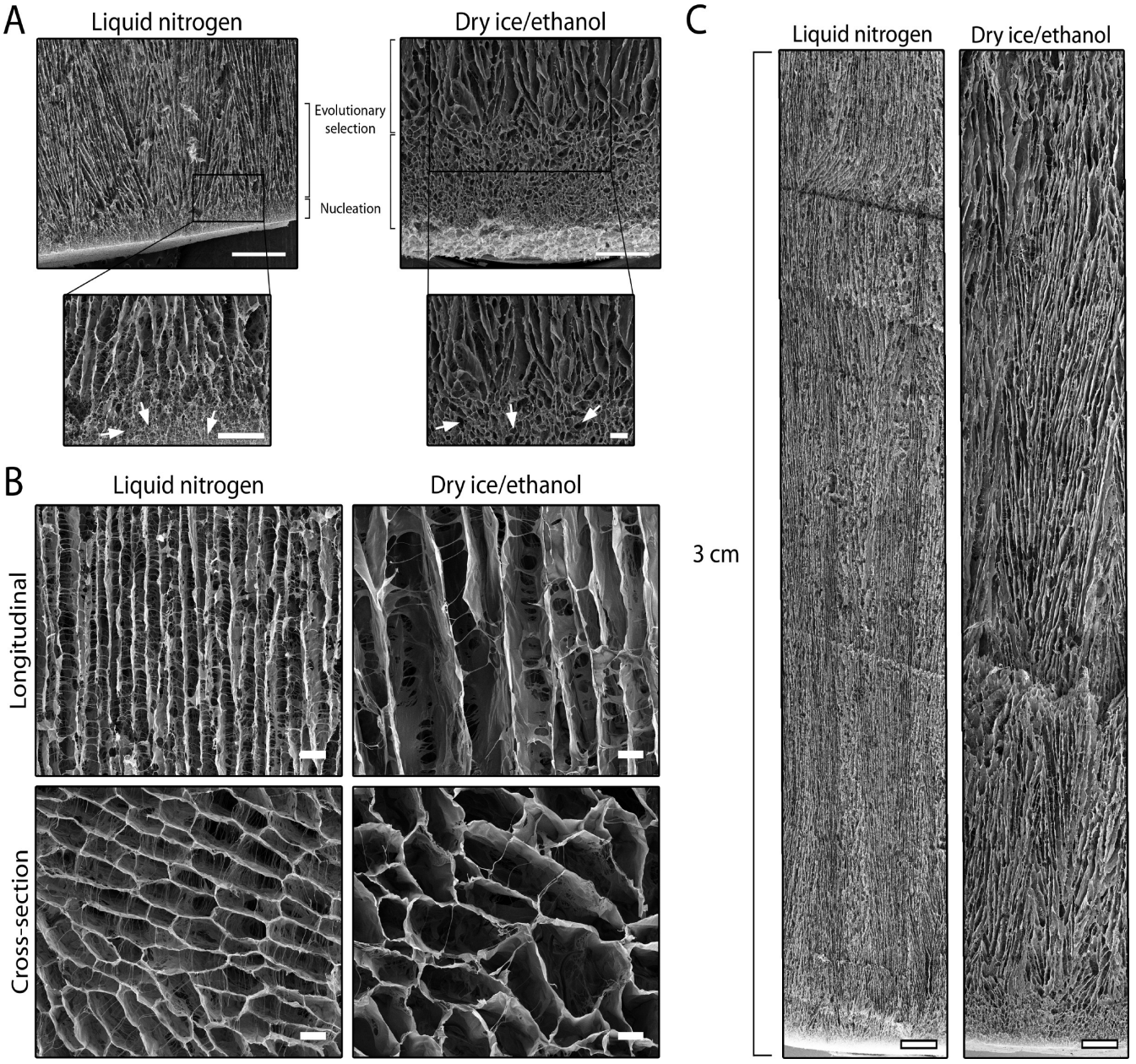

Figure 3. Scanning electron microscopical characterization of scaffolds constructed by freezing with liquid nitrogen or a mixture of dry ice and ethanol. (A) Round pores (arrows) were present at the base of the scaffolds, indicating ice crystal nucleation. Elongated pores in different directions were present above the area of nucleation, indicating evolutionary selection. The area of nucleation and evolutionary selection appears smaller in the case of freezing with liquid nitrogen compared to a mixture of dry ice and ethanol. (B) High magnification of the unidirectional pore structures in a longitudinal and cross-sectional view. The pores have a hexagonal/elliptic morphology, and are smaller with higher freezing speed (−196 °C: 66 ± 11 μm and −78 °C: 146 ± 30 μm, $p < 0.0001$). (C) Panorama views of longitudinal sections of unidirectional scaffolds made using a 30 mL collagen suspension. Unidirectional pores run from bottom to top over a length of >25 mm. Scale bars in the main figure of part A are 1 mm and in close-ups 300 μm, in B 100 μm, and in C 1 mm.

temperature gradient sensors were placed on the aluminum surface at three different locations. The sensor located on the thick aluminum part of the wedge always showed a lower temperature compared to sensors placed midway and on the thin aluminum part. The temperature difference between the left and right sensor was 1.1 ± 0.9 °C ($p < 0.0001$) and 0.3 ± 0.1 °C ($p < 0.0001$) for −196 and −78 °C, respectively, resulting in temperature differences of 0.3 ± 0.3 and 0.1 ± 0.0 °C/cm. This indicates the presence of a significant horizontal temperature gradient from left to right over the aluminum surface of the wedge system during the freezing process, for freezing at −196 as well as at −78 °C. Temperature measurements performed using the nonwedge, flat system did not reveal an obvious temperature differences between different horizontal locations.

3.2. Scaffold Characterization. Directional freezing and lyophilization was applied to construct scaffolds with unidirectional pores. The collagen scaffolds constructed using the standard method (with 10 mL collagen suspension) comprised a height of 12 mm. In the lower parts of the scaffolds, SEM images (Figure 3A) indicated a small area of round pores at the base of the freeze-dried scaffolds. Above this area, there was a small area where elongated pores were present in multiple directions. These

DOI: 10.1021/acsami.5b00169
ACS Appl. Mater. Interfaces 2015, 7, 8495−8505

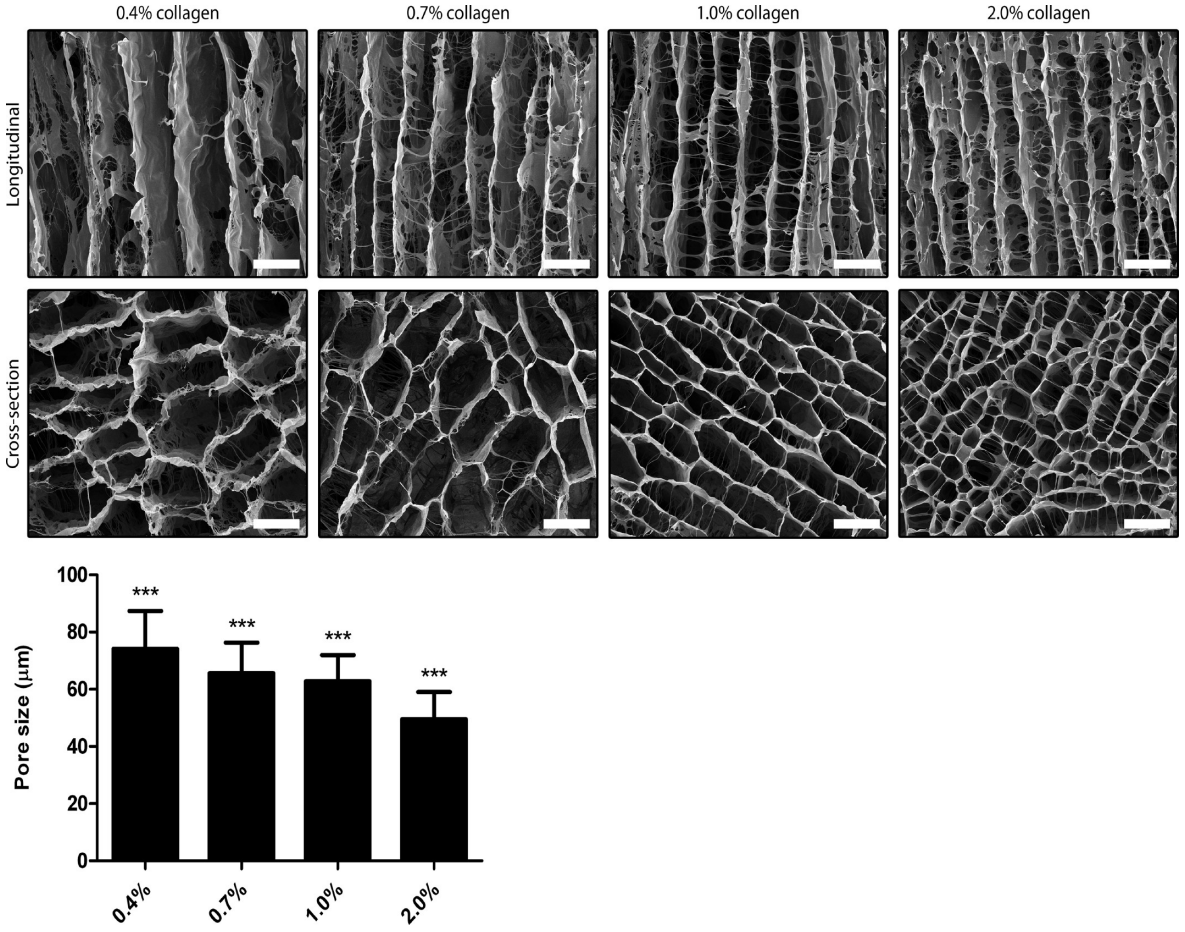

Figure 4. Scaffolds constructed from suspensions with different collagen concentrations. Scaffolds with unidirectional pores could be prepared for all applied collagen concentrations. Hexagonal/elliptic pores in the scaffolds were observed, with no apparent differences in wall thickness. An increase in collagen concentration resulted in an increase in the number of pores and a decrease in pore size (***: $p < 0.0001$). Scale bars represent 100 μm.

observations indicate an initial process of nucleation and evolutionary selection (see the Discussion). The height of the nonunidirectional area was less for higher freezing speeds, i.e., 2 and 3 mm for −196 and −78 °C, respectively. Above the nonunidirectional area (2 mm in height), unidirectional pores were present throughout the scaffold from base to top over a distance of 10 mm (Figure 3B). The cross sections of scaffolds (Figure 3B) showed a honeycomb-like morphology of the pores with small openings in the pore walls. These openings provide interconnectivity between adjacent pores. Furthermore, thin thread-like struts bridging opposite pore walls were observed in both longitudinal and cross sections.

Scaffolds with a height of over 30 mm were constructed from a 30 mL collagen suspension using freezing at −196 and −78 °C (Figure 3C). These scaffolds contained unidirectional pores over a length of about 28 mm.

3.3. Control of Pore Morphology. For an overview of the parameters examined and results obtained see Table 1.

3.3.1. Freezing Temperature. Pore sizes in scaffolds could be affected by freezing temperature: a fast freezing process using liquid nitrogen resulted in smaller pores compared to freezing using a mixture of dry ice and ethanol (66 ± 11 μm for −196 °C: 146 ± 30 μm for −78 °C, $p < 0.0001$).

3.3.2. Collagen Concentration. Scaffolds with aligned unidirectional pores were constructed using four collagen concentrations. Pore diameters were affected by collagen concentration (Figure 4) and were 74 ± 13, 66 ± 11, 63 ± 9, and 50 ± 10 μm in 0.4, 0.7, 1.0, and 2.0% scaffolds, respectively ($p < 0.0001$). For all collagen concentrations, honeycomb-like pores were observed in the scaffolds with no apparent differences in wall thickness. Although no mechanical tests were performed, handleability of the scaffolds improved with increased collagen concentration.

3.3.3. Incorporation of Detergents. Production of scaffolds from a collagen suspension in 15 mM octyl β-D-glycopyranoside in 0.25 M acetic acid also resulted in unidirectional collagen scaffolds after freezing and lyophilization. The wall structure was similar to scaffolds prepared using 0.25 M acetic acid without this nonionic detergent, but a decrease in pore size from 66 ± 11 to 57 ± 10 μm was noted ($p < 0.0001$, results not shown).

3.3.4. Concentration of Acetic Acid. Unidirectional collagen scaffolds could be constructed from collagen suspensions with different concentrations of acetic acid. For reference, collagen fibrils were incubated in Milli-Q water. The pores in these scaffolds consisted of thread-like structures and thin walls. SEM images indicated that the unidirectional pore structure was present, although somewhat masked by the highly thread-like structure. Morphologically, scaffolds prepared using collagen suspended in 0.025 M acetic acid resembled the structure of scaffolds prepared using collagen suspended in Milli-Q water (Figure 5). When increasing the concentration of acetic acid from 0.025 to 0.25 M acetic acid, scaffolds became less filamentary and the wall structure was more closed. A further increase of the acetic acid concentration from 0.25 to 2 M acetic

DOI: 10.1021/acsami.5b00169
ACS Appl. Mater. Interfaces 2015, 7, 8495−8505

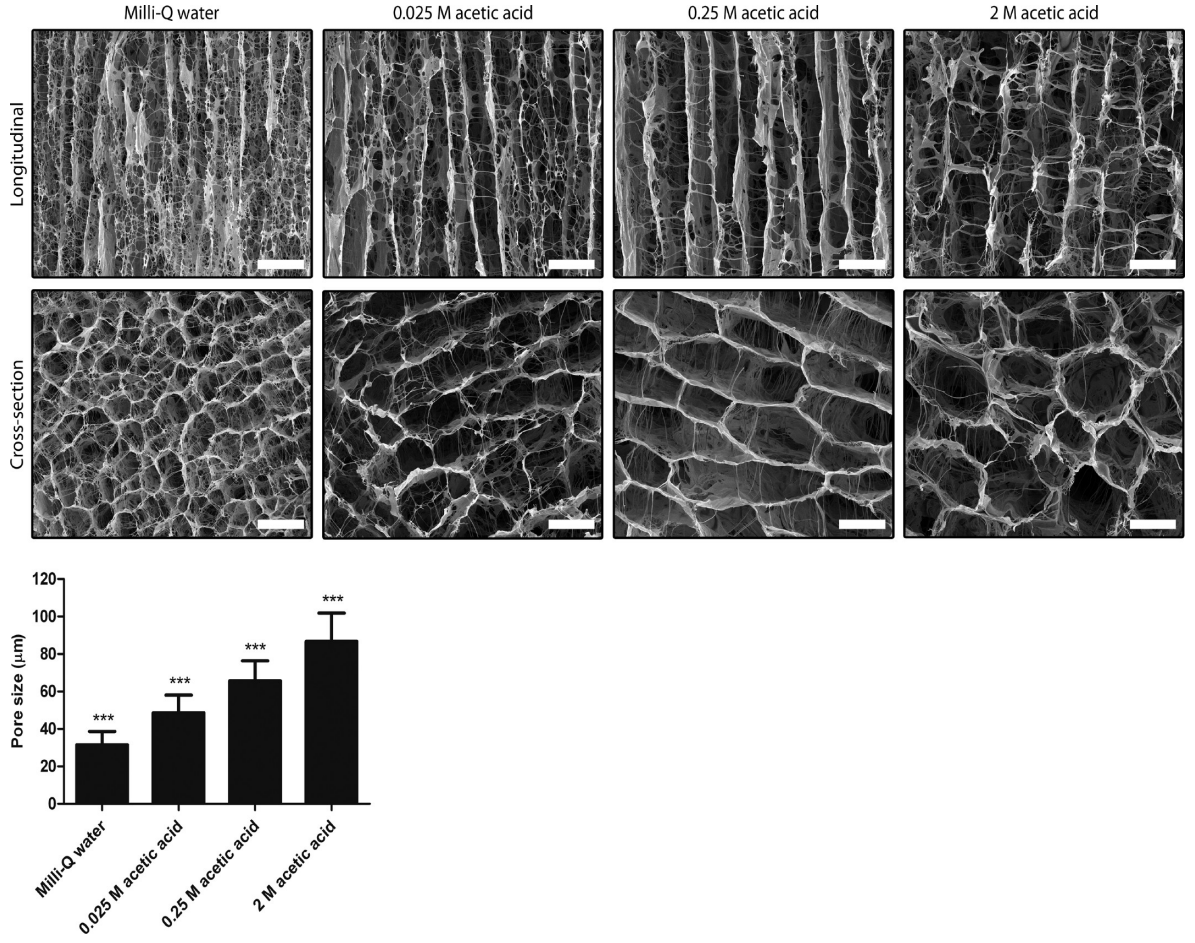

Figure 5. Unidirectional collagen scaffolds prepared from collagen suspensions with different concentrations of acetic acid. An increase in the concentration of acetic acid resulted in scaffolds with a less thread-like more closed wall structure and increased pore sizes (***: $p < 0.0001$). Scale bars represent 100 μm.

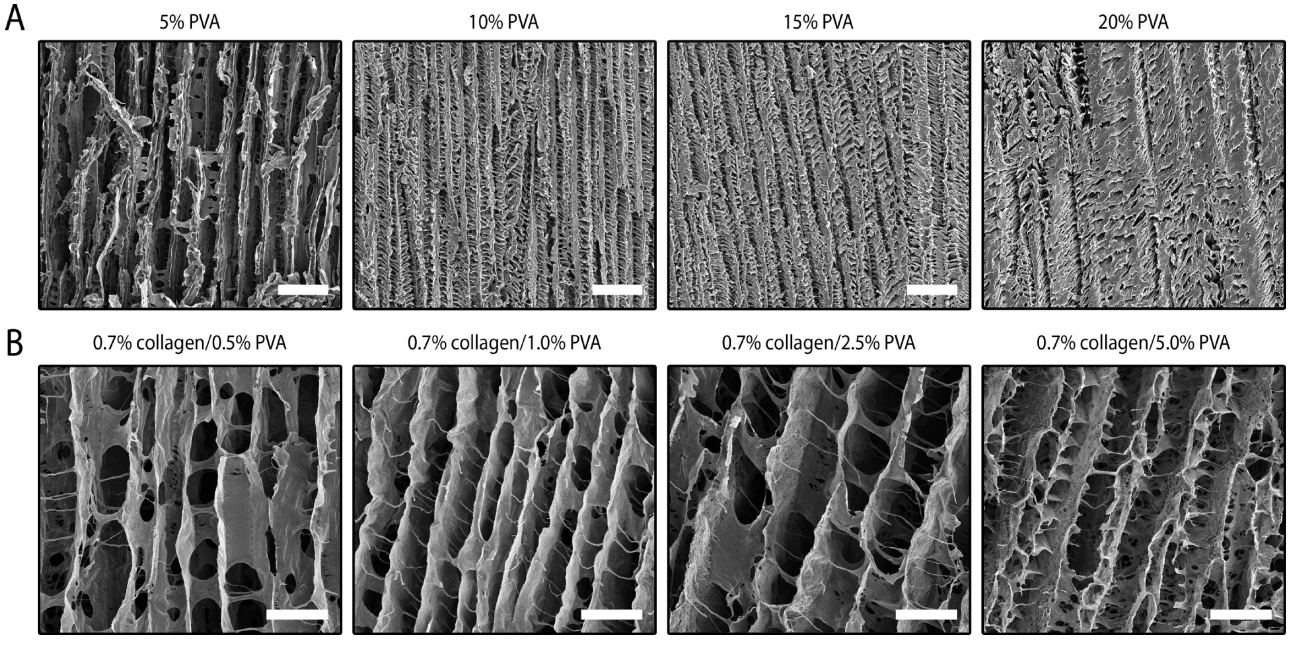

Figure 6. Versatility of the wedge system: unidirectional scaffolds prepared from poly(vinyl alcohol) (PVA, a synthetic polymer), and collagen + PVA. (A) Longitudinal sections of unidirectional scaffolds prepared with various concentrations of PVA. The unidirectional pore structure was observed for all concentrations. Pore sizes decreased with increasing concentrations of PVA. (B) Longitudinal sections of unidirectional hybrid collagen-PVA scaffolds. A mixed morphology resembling features from both collagen and PVA scaffolds was observed. Scale bars represent 100 μm.

DOI: 10.1021/acsami.5b00169
ACS Appl. Mater. Interfaces 2015, 7, 8495−8505

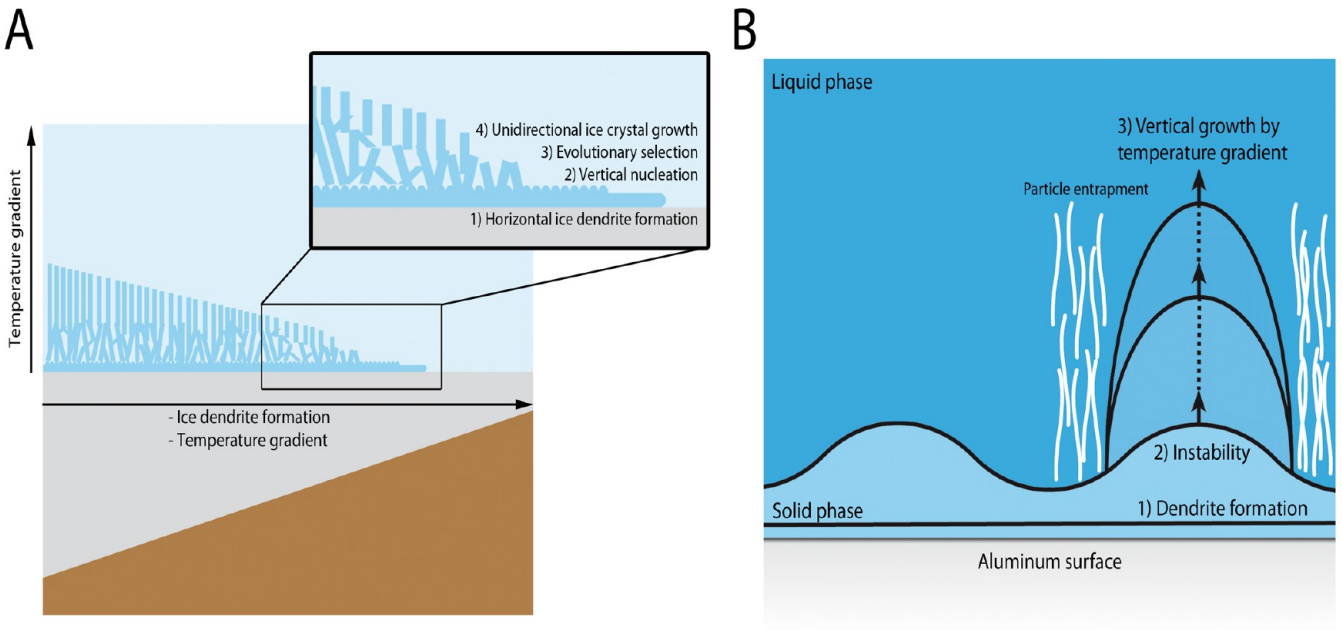

Figure 7. Proposed physical principles underlying the formation of aligned unidirectional scaffolds. (A) Schematic representation of the physical processes occurring during directional solidification, resulting in unidirectional ice crystal growth. The direction of the growing ice front is facilitated by the wedges, providing a controlled solidification area for ice dendrites. Nucleation sites develop, which merge into ice crystals by evolutionary selection,[27] and grow upward due to the vertical temperature gradient. The horizontal temperature gradient, facilitated by the wedge shape, may stabilize the formation of aligned unidirectional ice crystals. (B) The planar ice surface progresses into an unstable surface as the result of physical disturbances in freezing media. Ice crystals grow out from protrusions or nuclei formed by these instabilities. Growth of ice crystals is guided by the vertical temperature gradient. Collagen fibrils and other particles are entrapped between the growing ice crystals. Panel B was adapted from Deville et al.[30] Copyright Wiley-VCH Verlag GmbH & Co. KGaA. Reproduced with permission.

acid further reduced the fibrillar nature of the scaffolds with an even more closed wall structure. The scaffolds showed no obvious differences in wall thickness. The pore sizes in the scaffolds were 32 ± 7, 49 ± 9, 66 ± 11, and 87 ± 15 μm for Milli-Q water, 0.025, 0.25, and 2 M acetic acid ($p < 0.0001$), respectively.

3.4. Application of System to Other (Bio)molecules. To evaluate the general applicability of the system, scaffolds with unidirectional pores were constructed using another protein (albumin), a synthetic polymer (PVA), or a mixture of a protein + polymer (collagen + PVA). The unidirectional pore orientation was clearly observed in scaffolds constructed from albumin. Albumin-based scaffolds displayed similar characteristics as those made from collagen, including a small area at the base of the scaffold of rounded pores and elongated pores in different directions (data not shown). Above this nonunidirectional area, unidirectional pores were present. The cross sections showed that the pores were irregular and oblong shaped. In general, albumin scaffolds consisted of smooth wall structures with additional globular structures.

Freezing of PVA suspensions at varying polymer concentration also resulted in scaffolds with unidirectional pores (Figure 6A). Morphologically, the wall structure resembled a fishbone-like arrangement, and an increase in polymer concentration resulted in a decrease in pore size with an increase in wall thickness.

Hybrid unidirectional scaffolds were constructed using 0.7% (w/v) collagen in combination with different concentrations of PVA: 0.5%, 1.0%, 2.5%, and 5% (w/v) (Figure 6B). The structure of hybrid scaffolds containing 5% PVA showed a mixed morphology combining the architecture observed for 5% PVA and 0.7% collagen scaffolds. The walls of hybrid scaffolds were thicker compared to those seen in collagen-only scaffolds. Moreover, a more fibred morphology was present in hybrid scaffolds compared to polymer-only scaffolds due to the addition of collagen, especially in the fibers crossing the pores. With lowered concentrations of PVA, the structure shifted to that observed for collagen scaffolds. The handleability of the scaffolds was improved by the incorporation of PVA compared to collagen scaffolds.

4. DISCUSSION

Large collagen scaffolds with unidirectional pore architecture were constructed by freezing collagen suspensions using liquid nitrogen or a mixture of dry ice and ethanol, applying a wedge-like construct consisting of both a thermal conductor and insulator. The delayed freezing process by the insulator may have aided in the development of crack-free scaffolds, whereas cracks were observed after fast freezing of collagen suspensions in metal casts in direct contact with liquid nitrogen. Moreover, changing the materials of the metal wedge and insulator to materials with different thermal conductivities may allow adaptation of ice crystal growth.[24] The wedge shape induced a small but significant horizontal temperature gradient, likely facilitating local nucleation at the coldest point, followed by laterally directed ice crystal growth over the metal surface which stabilizes unidirectional crystal growth. The horizontal temperature gradient may have introduced small differences in height between adjacent upward growing ice crystals, thereby blocking inclined growing of ice crystals, and resulting in a stabilized upward growth of ice crystals (Figure 7). A steeper angle of the wedge may give rise to a larger horizontal temperature gradient and thus improved stabilized unidirectional crystal growth.

DOI: 10.1021/acsami.5b00169
ACS Appl. Mater. Interfaces 2015, 7, 8495−8505

Four steps can be identified during the formation of unidirectional collagen scaffolds as based on optical observations, temperature measurements, and SEM analyses (Figure 7): (1) formation of a horizontally oriented network of ice dendrites, (2) development of vertical protrusions and/or nuclei, (3) evolutionary selection of the vertical growth direction, and (4) unidirectional (mainly cellular) ice crystal growth. Step 1: At the interface between the aluminum surface and collagen suspension, the ice nuclei that rapidly become dendrites protrude horizontally. The dendrites initially form at the coldest part of the wedge (the thick aluminum part) and spread over the aluminum surface, owing to the horizontal temperature gradient realized by the wedge-shaped metal. The horizontal temperature gradient thus provides a controlled solidification area for ice dendrites. Step 2: On top of the initial planar layer of dendrites, upward pointing protrusions may form on the ice dendrite arms as a result of morphological (so-called Mullins-Sekerka) instabilities.[25] An alternative possibility is a preferential heterogeneous nucleation of upward pointing ice crystallites on the dendrite arms. These nucleation sites left a mark as round pored structures at the base of the scaffolds (Figure 3). The nucleation mechanisms and crystal growth phenomena have recently been reviewed by Pawelec and co-workers.[26] Step 3: Evolutionary selection takes place in which only a selection of growing ice crystals will continue and form the structure of the unidirectional scaffold, protruding upward from the aluminum surface.[27] During evolutionary selection nonperpendicular growing ice crystal needles collide with perpendicular growing needles and stop growing. Only perpendicular growing ice crystals survive and continue growing. This process is likely the result of the combined vertical and horizontal temperature gradient. A similar mechanism was observed by Pawelec et al., demonstrating the transformation from isotropic (nucleation sites), via evolutionary selection, to growth of aligned pores upward. The nonunidirectional area was present throughout the whole sample, which may be addressed to the slow freezing applied, while in our experiments relatively fast-freezing was used.[28] Step 4: the further unidirectional upward cellular growth of the ice crystals after evolutionary selection is supported by the vertical temperature gradient. During freezing of the collagen suspension, ice and collagen/acetic acid/water compartments are formed. Aqueous acetic acid is a eutectic system (eutectic point: −26.7 °C, at a 60% (v/v) acetic acid to water ratio),[29] which results in compartmentalization during the freezing process: a compartment of frozen water and a compartment with concentrated liquid acetic acid in which the collagen fibers can be found (we assume that the collagen fibrils do not affect the eutectic point or the freezing process).

After lyophilization, pores showed a honeycomb-like morphology with thin bridging structures and openings in the wall. The development of the honeycomb-like structure can be explained by stacking of dendrites during cellular growth and the bridging structures by dendrite growth.[19] Openings in the wall structure are explained by the formation of side branches of ice crystals (branching phenomenon). These ice protrusions result in a continuous-interpenetrating network of ice crystals intertwined with collagen.[31] The characterization of the scaffolds indicated homogeneous pore size distributions throughout the scaffolds, whereas other studies often describe a gradual increase in pore size upward.[28,32] Since the basis of the unidirectional collagen scaffolds preparation is the formation and growth of ice crystals, manipulation of ice crystal growth offers possibilities to control scaffold parameters such as pore size and wall morphology, thus facilitating the construction of a range of collagen scaffolds with different characteristics.

Fast freezing using liquid nitrogen resulted in smaller pore sizes compared to slower freezing using a mixture of dry ice and ethanol. This complies with the well-known fact that dimensions of growing ice crystals generally decrease with increasing growth velocity.[33] Similar effects of the freezing rate on pore size have been reported extensively in literature.[9,12] The thermal conductivity of the materials used is an important parameter. For instance, Schoof et al.,[19] reported pore sizes of approximately 23 μm for collagen in 1.5 wt % acetic acid (resembling approximately 0.25 M acetic acid) frozen using copper blocks at a temperature of −180 °C, whereas Madaghiele et al.[2] reported pore sizes of 33 μm for collagen in hydrochloric acid frozen using liquid-nitrogen-cooled copper blocks, while we measured pore sizes of 66 μm for freezing with liquid nitrogen. The insulator applied in our experiments delayed the freezing process and attributed to the larger pore size.

Unidirectional collagen scaffolds were constructed with various collagen concentrations where an increase in collagen concentration resulted in a slight decrease in pore size. Similar trends were shown by Madaghiele et al. where an increase in collagen concentration from 0.5% to 2% (in hydrochloric acid) frozen with liquid nitrogen resulted in a decreased pore size from 33 to 23 μm after lyophilization.[2] This result is in agreement with data shown by Pawelec et al. where 0.5% and 1% collagen scaffolds contained respectively pore sizes of 120−170 and 90−160 μm.[28]

Next to freezing temperature and collagen concentration, ice crystal growth was influenced by detergents, such as octyl β-D-glycopyranoside, which tend to accumulate at the interface between the two phases (the solid (ice) and liquid (suspension) phases) where they decrease the surface energy (tension) to facilitate nucleation, resulting in smaller pores.[34]

The properties of the suspension medium also influenced pore size in unidirectional scaffolds. Collagen scaffolds made from increasing concentrations of acetic acid resulted in scaffolds with larger pore sizes, in line with observations made by Schoof et al., who also showed that an increase in acetic acid concentration resulted in an increase in pore size (20−40 um for 1.5−3.8 wt %).[19]

Unidirectional scaffolds have been constructed from other proteins than collagen and albumin, e.g., Zhang et al. prepared unidirectional scaffolds from silk fibroin and showed that an increase in silk fibroin concentration resulted in a decreased pore size, an improved pore orientation and an increased wall thickness.[10] Similar trends were described regarding PVA scaffolds by Gutiérrez et al.[35] In our experiments, the increased wall thickness was only observed for scaffolds prepared using BSA and PVA but not for collagen scaffolds, suggesting that different proteins/particles can be present varying compactness that influences ice crystal formation.

In this study, hybrid collagen/polymer scaffolds were prepared by mixing collagen and PVA prior to freezing and lyophilization. This method allows the freezing process to be the determining parameter for the final scaffold architecture. Other studies have created hybrid constructs by combining polymer meshes with hydrogels[36] or with a collagen/chitosan suspension prior to freeze-drying.[37] A limitation of such a strategy is that the meshes may have an effect on ice crystal growth during freezing and thus on the final pore structure of the freeze-dried scaffold.

Tissue engineering strategies generally encompass the use of scaffolds as cell-carriers and the incorporation of effector

DOI: 10.1021/acsami.5b00169
ACS Appl. Mater. Interfaces 2015, 7, 8495−8505

molecules to direct cellular ingrowth and differentiation.[24,38] Unidirectional collagen scaffolds may provide improved cellular ingrowth as the result of the unidirectional architecture.[1,31] An application for these scaffolds may be the regeneration of articular cartilage. Stimuli such as SDF-1α and growth factors of the BMP family may be coupled to the scaffold to attract mesenchymal stromal cells from the underlying subchondral bone and induce chondrogenesis, while the architecture facilitates migration of cells throughout the scaffold.[39,40]The incorporation of (biodegradable) polymers is an option to improve the mechanical strength of collagen scaffolds, as indicated in this study for PVA, a FDA approved, biocompatible, and water-soluble polymer. Especially for load-bearing applications, an improvement of the mechanical strength is required to develop long-lasting implants.[36]

The custom-made wedge system presented here allows a wide range of unidirectional scaffolds to be created in a simple manner and at low cost.

5. CONCLUSION

Porous scaffolds with unidirectional anisotropic pores were constructed by directional freezing using a custom-made wedge system. The mechanism of unidirectional ice crystal growth was elucidated, and ice crystal growth was manipulated to develop a wide range of unidirectional collagen scaffolds with distinctive pore structures.

■ ASSOCIATED CONTENT

Supporting Information

The process of planar ice dendrite formation visualized by video capture. This material is available free of charge via the Internet at http://pubs.acs.org.

■ AUTHOR INFORMATION

Corresponding Author

*E-mail: Michiel.Pot@radboudumc.nl. Tel.: +31243614304. Fax: +31243616413.

Present Addresses

[§]Department of Chemistry, College of Education, University of Salahaddin, Zanko Street, Erbil-Kurdistan Region, Iraq.

[∥]Physics Department, Faculty of Science, Ain Shams University, Cairo, Egypt.

Author Contributions

The manuscript was written through contributions of all authors. All authors have given approval to the final version of the manuscript.

Notes

The authors declare no competing financial interest.

■ ACKNOWLEDGMENTS

We thank the Technical Support Group from the Radboud Faculty of Social Sciences at the Radboud University for manufacturing of the aluminum and Obomodulan wedges. We also thank Erik de Ronde and Wil Corbeek for the technical support during conducting the experiments at the department of Solid State Chemistry, Institute for Molecules and Materials, Radboud University Nijmegen. We also acknowledge the Microscopic Imaging Centre for facilitating electron microscopy equipment (Radboud university medical center, Nijmegen, The Netherlands). This work was supported by a grant from the Dutch government to The Netherlands Institute for Regenerative Medicine (NIRM, grant No. FES0908).

■ ABBREVIATIONS

BSA, bovine serum albumin
PVA, poly(vinyl alcohol)
SEM, scanning electron microscopy

■ REFERENCES

(1) de Mulder, E. L. W.; Buma, P.; Hannink, G. Anisotropic Porous Biodegradable Scaffolds for Musculoskeletal Tissue Engineering. *Materials* **2009**, *2*, 1674−1696.

(2) Madaghiele, M.; Sannino, A.; Yannas, I. V.; Spector, M. Collagen-Based Matrices with Axially Oriented Pores. *J. Biomed. Mater. Res., Part A* **2008**, *85*, 757−767.

(3) Stokols, S.; Tuszynski, M. H. Freeze-Dried Agarose Scaffolds with Uniaxial Channels Stimulate and Guide Linear Axonal Growth Following Spinal Cord Injury. *Biomaterials* **2006**, *27*, 443−451.

(4) Wu, X.; Liu, Y.; Li, X.; Wen, P.; Zhang, Y.; Long, Y.; Wang, X.; Guo, Y.; Xing, F.; Gao, J. Preparation of Aligned Porous Gelatin Scaffolds by Unidirectional Freeze-Drying Method. *Acta Biomater.* **2010**, *6*, 1167−1177.

(5) de Mulder, E. L.; Hannink, G.; van Kuppevelt, T. H.; Daamen, W. F.; Buma, P. Similar Hyaline-Like Cartilage Repair of Osteochondral Defects in Rabbits Using Isotropic and Anisotropic Collagen Scaffolds. *Tissue Eng., Part A* **2014**, *20*, 635−645.

(6) Bhattacharjee, M.; Miot, S.; Gorecka, A.; Singha, K.; Loparic, M.; Dickinson, S.; Das, A.; Bhavesh, N. S.; Ray, A. R.; Martin, I.; Ghosh, S. Oriented Lamellar Silk Fibrous Scaffolds to Drive Cartilage Matrix Orientation: Towards Annulus Fibrosus Tissue Engineering. *Acta Biomater.* **2012**, *8*, 3313−3325.

(7) McCullen, S. D.; Autefage, H.; Callanan, A.; Gentleman, E.; Stevens, M. M. Anisotropic Fibrous Scaffolds for Articular Cartilage Regeneration. *Tissue Eng., Part A* **2012**, *18*, 2073−2083.

(8) Kroehne, V.; Heschel, I.; Schugner, F.; Lasrich, D.; Bartsch, J. W.; Jockusch, H. Use of a Novel Collagen Matrix with Oriented Pore Structure for Muscle Cell Differentiation in Cell Culture and in Grafts. *J. Cell. Mol. Med.* **2008**, *12*, 1640−1648.

(9) Caliari, S. R.; Harley, B. A. The Effect of Anisotropic Collagen-GAG Scaffolds and Growth Factor Supplementation on Tendon Cell Recruitment, Alignment, and Metabolic Activity. *Biomaterials* **2011**, *32*, 5330−5340.

(10) Zhang, Q.; Zhao, Y.; Yan, S.; Yang, Y.; Zhao, H.; Li, M.; Lu, S.; Kaplan, D. L. Preparation of Uniaxial Multichannel Silk Fibroin Scaffolds for Guiding Primary Neurons. *Acta Biomater.* **2012**, *8*, 2628−2638.

(11) Feng, C. H.; Cheng, Y. C.; Chao, P. H. The Influence and Interactions of Substrate Thickness, Organization and Dimensionality on Cell Morphology and Migration. *Acta Biomater.* **2013**, *9*, 5502−5510.

(12) Faraj, K. A.; van Kuppevelt, T. H.; Daamen, W. F. Construction of Collagen Scaffolds that Mimic the Three-Dimensional Architecture of Specific Tissues. *Tissue Eng.* **2007**, *13*, 2387−2394.

(13) Davidenko, N.; Gibb, T.; Schuster, C.; Best, S. M.; Campbell, J. J.; Watson, C. J.; Cameron, R. E. Biomimetic Collagen Scaffolds with Anisotropic Pore Architecture. *Acta Biomater.* **2012**, *8*, 667−676.

(14) Chen, M. C.; Sun, Y. C.; Chen, Y. H. Electrically Conductive Nanofibers with Highly Oriented Structures and Their Potential Application in Skeletal Muscle Tissue Engineering. *Acta Biomater.* **2013**, *9*, 5562−5572.

(15) Cheng, X.; Gurkan, U. A.; Dehen, C. J.; Tate, M. P.; Hillhouse, H. W.; Simpson, G. J.; Akkus, O. An Electrochemical Fabrication Process for the Assembly of Anisotropically Oriented Collagen Bundles. *Biomaterials* **2008**, *29*, 3278−3288.

(16) Sharma, S.; Panitch, A.; Neu, C. P. Incorporation of an Aggrecan Mimic Prevents Proteolytic Degradation of Anisotropic Cartilage Analogs. *Acta Biomater.* **2013**, *9*, 4618−4625.

(17) Stokols, S.; Tuszynski, M. H. The Fabrication and Characterization of Linearly Oriented Nerve Guidance Scaffolds for Spinal Cord Injury. *Biomaterials* **2004**, *25*, 5839−5846.

DOI: 10.1021/acsami.5b00169
ACS Appl. Mater. Interfaces 2015, 7, 8495−8505

(18) Wegst, U. G.; Schecter, M.; Donius, A. E.; Hunger, P. M. Biomaterials by Freeze Casting. *Philos. Trans. R. Soc., A* **2010**, *368*, 2099−2121.
(19) Schoof, H.; Apel, J.; Heschel, I.; Rau, G. Control of Pore Structure and Size in Freeze-dried Collagen Sponges. *J. Biomed. Mater. Res.* **2001**, *58*, 352−357.
(20) Zhang, H.; Hussain, I.; Brust, M.; Butler, M. F.; Rannard, S. P.; Coper, A. I. Aligned Two- and Three-Dimensional Structures by Directional Freezing of Polymers and Nanoparticles. *Nat. Mater.* **2005**, *4*, 787−793.
(21) O'Brien, F. J.; Harley, B. A.; Yannas, I. V.; Gibson, L. Influence of Freezing Rate on Pore Structure in Freeze-Dried Collagen-GAG Scaffolds. *Biomaterials* **2004**, *25*, 1077−1086.
(22) Ng, K. W.; Torzilli, P. A.; Warren, R. F.; Maher, S. A. Characterization of a Macroporous Polyvinyl Alcohol Scaffold for the Repair of Focal Articular Cartilage Defects. *J. Tissue Eng. Regener. Med.* **2014**, *8*, 164−168.
(23) Nillesen, S. T.; Geutjes, P. J.; Wismans, R.; Schalkwijk, J.; Daamen, W. F.; van Kuppevelt, T. H. Increased Angiogenesis in Acellular Scaffolds by Combined Release of FGF2 and VEGF. *J. Controlled Release* **2006**, *116*, e88−e90.
(24) Brouwer, K. M.; van Rensch, P.; Harbers, V. E.; Geutjes, P. J.; Koens, M. J.; Wijnen, R. M.; Daamen, W. F.; van Kuppevelt, T. H. Evaluation of Methods for the Construction of Collagenous Scaffolds with a Radial Pore Structure for Tissue Engineering. *J. Tissue Eng. Regener. Med.* **2011**, *5*, 501−504.
(25) Zhang, H. F.; Hussain, I.; Brust, M.; Butler, M. F.; Rannard, S. P.; Cooper, A. I. Aligned Two- and Three-Dimensional Structures by Directional Freezing of Polymers and Nanoparticles. *Nat. Mater.* **2005**, *4*, 787−793.
(26) Pawelec, K. M.; Husmann, A.; Best, S. M.; Cameron, R. E. Ice-Templated Structures for Biomedical Tissue Repair: From Physics to Final Scaffolds. *Appl. Phys. Rev.* **2014**, *1*, 021301−021313.
(27) van der Drift, A. Evolutionary Selection, a Principle Governing Growth Orientation in Vapour-Deposited Layers. *Philips Res. Rep.* **1967**, *22*, 267−288.
(28) Pawelec, K. M.; Husmann, A.; Best, S. M.; Cameron, R. E. Understanding Anisotropy and Architecture in Ice-Templated Biopolymer Scaffolds. *Mater. Sci. Eng., C* **2014**, *37*, 141−147.
(29) Landolt, H.; Börnstein, R. *Numerical Data and Functional Relationships in Science and Technology*, 6 ed.; Springer: Berlin, 1962; Vol. 2.
(30) Deville, S. Freeze-Casting of Porous Ceramics: A Review of Current Achievements and Issues. *Adv. Eng. Mater.* **2008**, *10*, 155−169.
(31) Barr, S. A.; Luijten, E. Structural Properties of Materials Created Through Freeze Casting. *Acta Mater.* **2010**, *58*, 709−715.
(32) Yunoki, S.; Ikoma, T.; Tsuchiya, A.; Monkawa, A.; Ohta, K.; Sotome, S.; Shinomiya, K.; Tanaka, J. Fabrication and Mechanical and Tissue Ingrowth Properties of Unidirectionally Porous Hydroxyapatite/Collagen Composite. *J. Biomed. Mater. Res., Part B* **2007**, *80B*, 166−173.
(33) Billia, B.; Trivedi, R. *Handbook of Crystal Growth*; Hurle, D. T. J., Ed.; Elsevier: Amsterdam, The Netherlands, p 918.
(34) Bujan, M.; Sikiric, M.; Filipovic-Vincekovic, N.; Vdovic, N.; Garti, N.; Furedi-Milhofer, H. Effect of Anionic Surfactants on Crystal Growth of Calcium Hydrogen Phosphate Dihydrate. *Langmuir* **2001**, *17*, 6461−6470.
(35) Gutiérrez, M. C.; García-Carvajal, Z. Y.; Jobbágy, M.; Rubio, F.; Yuste, L.; Rojo, F.; Ferrer, M. L.; del Monte, F. Poly(vinyl alcohol) Scaffolds with Tailored Morphologies for Drug Delivery and Controlled Release. *Adv. Funct. Mater.* **2007**, *17*, 3505−3513.
(36) Schuurman, W.; Khristov, V.; Pot, M. W.; van Weeren, P. R.; Dhert, W. J.; Malda, J. Bioprinting of Hybrid Tissue Constructs with Tailorable Mechanical Properties. *Biofabrication* **2011**, *3*, 021001−021008.
(37) Haaparanta, A. M.; Jarvinen, E.; Cengiz, I. F.; Ella, V.; Kokkonen, H. T.; Kiviranta, I.; Kellomaki, M. Preparation and Characterization of Collagen/PLA, Chitosan/PLA, and Collagen/chitosan/PLA Hybrid Scaffolds for Cartilage Tissue Engineering. *J. Mater. Sci.: Mater. Med.* **2014**, *25*, 1129−1136.
(38) Efe, T.; Theisen, C.; Fuchs-Winkelmann, S.; Stein, T.; Getgood, A.; Rominger, M. B.; Paletta, J. R.; Schofer, M. D. Cell-free Collagen Type I Matrix for Repair of Cartilage Defects-Clinical and Magnetic Resonance Imaging Results. *Knee Surg. Sports Traumatol. Arthrosc.* **2012**, *20*, 1915−1922.
(39) Richter, W. Mesenchymal Stem Cells and Cartilage in Situ Regeneration. *J. Int. Med.* **2009**, *266*, 390−405.
(40) Mendelson, A.; Frank, E.; Allred, C.; Jones, E.; Chen, M.; Zhao, W.; Mao, J. J. Chondrogenesis by Chemotactic Homing of Synovium, Bone Marrow, and Adipose Stem Cells in Vitro. *FASEB J.* **2011**, *25*, 3496−3504.

DOI: 10.1021/acsami.5b00169
ACS Appl. Mater. Interfaces 2015, 7, 8495−8505